Analysis of genetic mosaics in developing and adult *Drosophila* tissues

Tian Xu and Gerald M. Rubin

Howard Hughes Medical Institute, and Department of Molecular and Cell Biology, University of California, Berkeley, California 94720, USA

SUMMARY

We have constructed a series of strains to facilitate the generation and analysis of clones of genetically distinct cells in developing and adult tissues of *Drosophila*. Each of these strains carries an FRT element, the target for the yeast FLP recombinase, near the base of a major chromosome arm, as well as a gratuitous cell-autonomous marker. Novel markers that carry epitope tags and that are localized to either the cell nucleus or cell membrane have been generated. As a demonstration of how these strains can be used to study a partic-ular gene, we have analyzed the developmental role of the *Drosophila* EGF receptor homolog. Moreover, we have shown that these strains can be utilized to identify new mutations in mosaic animals in an efficient and unbiased way, thereby providing an unprecedented opportunity to perform systematic genetic screens for mutations affecting many biological processes.

Key words: *Drosophila*, genetic mosaics, cell markers, FRT elements, genetic screens, EGF receptor

INTRODUCTION

In *Drosophila,* mosaic animals that bear clones of geneti-cally distinct somatic cells have been used to address many biological questions including autonomy of gene action, restriction of cell fate and growth pattern (reviewed by Postlethwait, 1976 and Ashburner, 1989). Gynandro-morphs, individuals mosaic for sexual identity that arise spontaneously as the result of the somatic loss of an X chro-mosome, were first recognized by T. H. Morgan (1914). Later, gynandromorphs produced at higher frequencies using unstable chromosomes or mutations that induce chro-mosomal loss were used to construct developmental 'fate maps', which plot the relative positions in the early embryo of precursor cells for structures that arise later in develop-ment (Garcia-Bellido and Merriam, 1969; Hotta and Benzer, 1972 and Kankel and Hall, 1976). In the past decades, several different approaches have been taken to generate mosaic animals including chromosomal loss, mitotic recombination, and cell or nuclear transplantation (Stern, 1936; also see reviews by Hall et al., 1976; Lawrence et al., 1986 and Ashburner, 1989). The most widely used method for generating mosaicism involves mitotic recombination between homologous chromosomes induced by ionizing radiation (e.g. X-rays; Patterson, 1929; Friesen, 1936). X-rays can be applied to somatic cells at specific developmental stages to cause rare chromosomal breaks, which lead to exchange between homologous chro-mosome arms, so that, after segregation at mitosis, a cell homozygous for the part of a chromosome arm distal to the point of recombination is formed. This cell will then divide and generate a clone of cells in the adult. The cells in this clone can be recognized if, as a consequence of the recom-bination event, cells in the clone become homozygous for a mutation that alters the morphology of the cuticle in a cell-autonomous fashion (reviewed by Hall et al., 1976; Lawrence et al., 1986 and Ashburner, 1989).

Although cuticular markers have been successfully used for analyzing external structures, they cannot be used to identify the genotype of cells in developing or internal tis-sues. The development of adult structures involves a series of developmental decisions which are made long before the eclosion of the adult, and many genes are involved in mul-tiple cellular processes in a given tissue during develop-ment. Thus, the interpretation of the role of a gene in a given developmental process based on the terminal pheno-type of mutant clones in the adult can often be misleading and one would like to analyze the behavior of clones of mutant cells during development. Enzymes for which cell-viable null alleles (Janning, 1972; Kankel and Hall, 1976) or temperature-sensitive alleles (Lawrence, 1981) and con-venient histochemical assays exist, have been used to mark some internal tissues. However, the general application of these enzyme markers has been limited by problems such as tissue specificity, developmental effects of enzyme loss, the resolution of the histochemical assay, and the chromo-somal location of the marker gene. The lack of universal cell markers for developing tissues has limited the use of genetic mosaics in addressing developmental questions, and impeded efforts to dissect genetically the structure and function of internal organs, such as the brain. To address these limitations, we have constructed genes encoding chimeric proteins that serve as gratuitous, cell-autonomous markers.

The low frequency of mosaicism produced by X-ray-induced mitotic recombination has also limited the use of

mosaic analysis in internal or developing tissues that require dissection and histology to detect clones of mutant cells. Recently, Golic and Lindquist (1989) have shown that the site-specific recombination system of the yeast 2 μm plasmid (the FLP recombinase and its target the FRT sequence) can function in *Drosophila*. Golic (1991) has further shown that this recombination system can be used to induce high frequency mitotic recombination between FRT sites located on homologous chromosome arms. In addition to somatic tissues, the FRT/FLP system has been shown to be functional in both male and female germ-line cells (Golic, 1991; Chou and Perrimon, 1992). The use of the FRT sequence to induce high frequency mosaicism for a particular gene requires that the FRT sequence be located closer to the centromere than the gene of interest. We have introduced dominantly marked FRT sequences into the genome near the centromere on each major chromosome arm. We have constructed chromosomes that carry cell markers or adult cuticular markers in addition to these FRTs. These chromosomes make it possible to perform mosaic analysis in both developing and adult tissues for more than 95% of *Drosophila* genes. They also provide a way of efficiently generating and screening mosaic animals for new mutations affecting many biological processes, including lethal mutations affecting the development and function of adult structures that would not be identified in most genetic screens.

MATERIALS AND METHODS

DNA constructs

P[ry+, hs-neo, FRT] was constructed by combining two 0.7 kb *Hin*dIII-*Bam*HI fragments that contain FRT sites (McLeod et al., 1984), a 7 kb *Hin*dIII fragment containing the *ry+* gene (Spradling and Rubin, 1983), and a second copy of the *hs-neo* gene into the pUCHsneo vector (Steller and Pirrotta, 1985) as diagrammed in Fig. 2A. *P[mini-w+, hs-ΔM]* was constructed by cloning a fragment containing the *hsp70* promoter and sequences encoding the ΔM chimeric protein into the *Xba*I site of the pCaSpeR-hs vector (Thummel and Pirrotta, 1992) as diagrammed in Fig. 1A. The ΔM chimeric protein is a fusion of the MYC epitope-containing peptide (Gln Gly Thr Glu Gln Lys Leu Ile Ser Glu Glu Asp Leu Asn stop; Evan et al., 1985) to amino acids 1-484 of the P-element transposase (Rio et al., 1986). *P[mini-w+, hs-NM]* was constructed by cloning a fragment encoding the NM chimeric protein between the *Xba*I and *Eco*RI sites of the pCaSpeR-hs vector (see Fig. 1A). The NM chimeric protein is a fusion of a 20 amino acid peptide, containing the same MYC epitope, to sequences of the Notch protein (amino acids 1-85 and 1466-1963; Wharton et al., 1985; Rebay et al., 1991). In addition to the ΔM and NM proteins, the ΔF protein in which the FLAG peptide (Asp Tyr Lys Asp Asp Asp Asp Lys stop; Hopp et al., 1988) replaced the MYC sequence in the ΔM protein was constructed. The *P[mini-w+, hs-ΔF]* construct was made by cloning a fragment containing the *hsp70* promoter and sequences encoding the ΔF chimeric protein into the *Xba*I site of the pCaSpeR 3 vector (Thummel and Pirrotta, 1992). Details of individual cloning steps for each of the constructs are available from the authors upon request. To assess the effect of marker proteins on development, larvae from three transformant lines of each of the cell marker constructs were incubated daily at 38°C for 60 minutes until the eclosion of the adult; no morphological defects were detected in these animals.

Fly strains, crosses and culture

P-element-mediated transformation of *Drosophila* was performed as described by Rubin and Spradling (1982). Independent *P[ry+, hs-neo, FRT]* transformant lines were established by mobilizing a *P[ry+, hs-neo, FRT]* element from a *CyO, P[ry+, hs-neo, FRT]* chromosome. The *hsFLP* construct was described by Golic and Lindquist (1989) and the *hsFLP* insertion on the *MKRS* chromosome was described by Chou and Perrimon (1992). The *P[ry+, y+]* construct was described by Geyer and Corces (1987) and the insertions on the autosomes were kindly provided by V. Corces (unpublished results). All other mutations and chromosomes are described by Lindsley and Zimm (1992). Unless otherwise indicated, all fly cultures and crosses were grown on standard fly medium at 25°C. All strains are *Drosophila melanogaster* and were produced by standard crosses. Strains listed in Table 1 have been deposited in the Bloomington Drosophila Stock Center. The strains carrying both *P[ry+, hs-neo, FRT]* and *hsFLP* insertions were kept at 18°C for at least 10 generations. No obvious defects were found in these strains.

Two copies of the *hs-neo* gene were placed in the *P[ry+, hs-neo, FRT]* construct to facilitate the genetic selection for this element. Flies carrying the *P[ry+, hs-neo, FRT]* element can be selected by their resistance to G418 (Geneticin, GIBCO laboratories). G418-containing medium was made as follows: a few holes were made in standard fly medium with toothpicks, and 0.2-0.3 ml of 25 mg/ml freshly made G418 solution was added per 10 ml of medium and the vials were allowed to air-dry for several hours. G418 is stable in medium stored at 4-18°C for more than 2 weeks. Five or six pairs of flies were allowed to lay eggs for 1-2 days in single vials. In crosses cultured at 25°C, heat-shock treatment of the larvae was not required for the selection. If crosses were cultured at a lower temperature, a 60 minute incubation in a 38°C water bath was required once or twice during early larval stages for the selection of neo^R flies.

P-elements can act as potent insertional mutagens and the resulting mutations are readily amenable to molecular characterization (reviewed by Rubin, 1985). Thus, it might be desirable to use P-elements as the mutagen in certain F_1 screens. However, when one mobilizes a P-element to mutagenize the genome, the *P[ry+, hs-neo, FRT]* elements that are essential for inducing mosaicism will often be removed from their original sites. To avoid this problem, we have tested the feasibility of crippling the *P[ry+, hs-neo, FRT]*; we selected for *ry⁻* flies after exposure to P-transposase in the hope that the 5′-P-element end in the original insert would be deleted together with the sequences of the adjacent *ry+* gene. We simultaneously selected for maintenance of the FRT sequences by requiring resistance to G418. We have tested this idea with three different *P[ry+, hs-neo, FRT]* insertions and in each case, *ry⁻* and neo^R resistant derivatives were obtained (data not shown). Further examination of these derivative *P[ry⁻, hs-neo, FRT]* insertions revealed that indeed some of them remained at their original insertion site and retained their ability to mediate mitotic recombination while their mobility was abolished or significantly decreased (data not shown).

The two *Egfr* alleles used in our experiments represent complete or nearly complete loss-of-function mutations: *Df(2R)Egfr^t18A* (*Df(2R)top^18A*) is a deficiency; the single polytene band in which the *Egfr* gene is located has been deleted (Price et al., 1989). The *Egfr^f3C81* (*flb^3C81*) mutation is an ethyl methane sulfonate (EMS)-induced strong *faint little ball* allele (Nüsslein-Volhard et al., 1984; Clifford and Schüpbach, 1989). Since the two alleles exhibit similar mutant phenotypes in our analyses, we use *Egfr⁻* and *Egfr+* to denote genetic loss of function and wild-type function for the locus, respectively. The dominant *Egfr* mutation used in our experiments, *Elp^B1* (*Egfr^EB1*), is described in Baker and Rubin (1989). The following fly strains were used in

the experiments with the *Egfr* shown in Figs 4 and 5: (1) w^{1118}, *hsFLP1; P[ry$^+$, hs-neo, FRT]43D, P[ry$^+$, w$^+$]47A*. (2) w^{1118}, *hsFLP1; P[ry$^+$, hs-neo, FRT]43D, P[mini-w$^+$, hs- M]45F*. (3) w^{1118}, *hsFLP1; P[ry$^+$, hs-neo, FRT]43D*. (4) w^{1118}, *hsFLP1; P[ry$^+$, hs-neo, FRT]43D, Egfr^{t3C81}/CyO*. (5) w^{1118}, *hsFLP1; P[ry$^+$, hs-neo, FRT]43D, Egfr^{EB1}/CyO*. (6) w^{1118}, *hsFLP1; P[ry$^+$, hs-neo, FRT]43D, P[mini-w$^+$, hs- M]45F, Egfr^{f3C81}/CyO*. Mosaic animals shown in the figures were obtained from crosses between the following strains: (2) and (4), (3) and (6) for Fig. 4; (1) and (5), (2) and (5) for Fig. 5.

Mosaic animals

To produce clones in the imaginal discs and in the adult cuticle, eggs from the appropriate crosses were collected for 12 hours, aged for another 24 hours, and vials containing these first instar larvae were then incubated in a 38°C water bath for 60 minutes to induce mitotic recombination. To induce mitotic recombination in third instar larvae, wandering third instar larvae were picked into new vials and then incubated in a 38°C water bath for 60 minutes. For producing mosaic ovaries, adult females from well-fed crosses were transferred into new vials, the cotton plugs were pushed down to restrict the movement of the flies, and the vials were then incubated in a 38°C water bath for 60 minutes 2.5 days before dissection.

To determine the frequency of mosaicism produced by each of the *P[ry$^+$, hs-neo, FRT]* insertions, first instar larvae (30-32 hours after egg laying) of the appropriate genotypes were incubated in a 38°C water bath. For the *P[ry$^+$, hs-neo, FRT]18A, 40A* and *43D* insertions, 0, 10, 20, 30, 40, 50 and 60 minute incubations were performed; for the other insertions only the 0 and 60 minute incubations were performed.

Histology and immunocytochemistry

Staining of imaginal discs was performed as follows: vials containing wandering third instar larvae were incubated in a 38°C water bath for 60-90 minutes to induce the expression of marker proteins. Larvae were returned to a 25°C incubator for 30-90 minutes before dissection on ice. Discs were then fixed for 40 minutes in PLP (2% paraformaldehyde, 0.01 M NaIO$_4$, 0.075 M lysine, 0.037 M sodium phosphate, pH 7.2) or for 20 minutes in 4% freshly made formaldehyde in 1× PBS on ice and then washed four times for 5 minutes each in PSN (0.037 M sodium phosphate, pH 7.2, 3% goat serum, 0.1% Saponin). Discs were then incubated for 2 hours at room temperature or overnight at 4°C with anti-MYC epitope mAb Myc 1-9E10.2 (Evan et al., 1985; c-*myc* (Ab-1), Oncogene Science) or anti-FLAG mAb M2 (gift of Steven Gillis, Immunex Inc.; also available from IBI) at a 1:100 dilution (1 μg/ml) in PSN. Discs were then washed four times in PSN and incubated with either FITC-, Texas Red- or HRP-conjugated goat anti-mouse IgG (Jackson Laboratories) at a 1:200 dilution in PSN. After a 2 hour incubation at room temperature, the discs were washed four times in PSN and then mounted in glycerol mount (90% glycerol, 1× PBS, 0.5% n-propyl gallate). For double labeling experiments, a FITC-conjugated goat anti-HRP IgG (Organon Teknika Corporation) was also added to the staining solution at a 1:500 dilution. After 2 hours incubation at room temperature, the discs were washed four times in PSN and then mounted in Glycerol mount. For ovary staining, adult females were incubated in a 38°C water bath for 60 minutes and were returned to a 25°C incubator for 90 minutes before dissection. Ovaries were fixed and stained as for imaginal discs. The M and NM markers have a short perdurance. After several divisions or 4 hours after the first induction (60 minutes at 38°C), the levels of the marker proteins have decreased so that they do not interfere with the detection of newly induced proteins. For staining of adult head sections, induction of the marker protein was carried out as for ovary staining.

The procedures for preparing and staining adult frozen sections were as described by Fortini and Rubin (1990) and the dilution conditions for the antibodies were the same as used for imaginal disc staining.

Adult eyes, heads and bodies were either placed in drops of water on top of a slide before photographing under a compound microscope or directly photographed under a dissecting microscope. Adult flies for scanning electron micrographs were prepared as described (Xu and Artavanis-Tsakonas, 1990).

Mutagenesis and F$_1$ screens

Four *82-1 F* males (Table 1) which were irradiated with X-rays (4000 r), mated to ten *82- M Sb y$^+$ F/TM3, Sb* virgins in each of 18 vials. Males were removed from the vials after 4 days while the females were allowed to lay eggs for another three days. Eggs from the females were collected every 24 hours and aged for another 24 hours before being incubated in a 38°C water bath for 60 minutes. F$_1$ individuals displaying mutant phenotypes in clones were collected and mated to *82- M Sb y$^+$ F/TM3, Sb* flies in separate vials to re-examine the clonal mutant phenotypes and to balance the induced mutations. For lines derived from male F$_1$ individuals, *TM3, Sb*-carrying *w$^-$* F$_2$ siblings were crossed to each other to obtain balanced stocks. For lines derived from female F$_1$ individuals, male F$_2$ offspring that carried mutant somatic clones were mated to *82- M Sb y$^+$ F/TM3, Sb* virgins to obtain balanced stocks.

Microscopy

Confocal images were collected using either a Bio-Rad MRC-600 system attached to a Zeiss Axiovert compound microscope or a Zeiss confocal microscope. Confocal images were photographed from a NEC MultiSync 3D color image monitor. Combined confocal images were made using the Merge software provided by Bio-Rad. Scanning electron micrographs were prepared on an International Scientific Instruments DS-130 SEM. Non-confocal photomicrographs were prepared using a Zeiss Axiophot microscope or a Nikon dissecting microscope.

RESULTS AND DISCUSSION

Cell markers for developing and internal tissues

In order to provide cell-autonomous markers whose expression can be induced in developing and internal tissues, we have constructed several novel chimeric genes and introduced them into the *Drosophila* genome. In choosing which chimeras to make, several features were considered desirable for such cell markers. First, the chimeric genes should be expressed in every cell in all developing and internal tissues. The *hsp70* promoter has been shown to be capable of directing expression of genes in nearly all cells of both developing and adult tissues after heat-shock treatment (Lis et al., 1983), so we placed all our marker genes under the control of the *hsp70* regulatory sequences (Fig. 1A). Second, the proteins expressed by the chimeric genes should be scorable at the level of individual cells. We have chosen to fuse short foreign peptides, which are recognized by commercially available monoclonal antibodies, to portions of known *Drosophila* proteins. The *Drosophila* proteins are designed to serve as carriers which will target the chimeric proteins to specific subcellular locations. Third, the marker proteins should have a short half life so that they do not persist for many cell divisions after removal of

the marker genes through mitotic recombination. Finally, the expression of the marker proteins should not interfere with normal development.

We have constructed two chimeric proteins with different subcellular locations. The πM protein is a fusion between a peptide (MYC) from the human c-*myc* protein (Evan et al., 1985) and the N-terminal sequence of the *Drosophila* P-element transposase (O'Hare and Rubin, 1983), which is targeted to nuclei (Fig. 1A,B). Cells expressing the πM protein can be visualized by staining with a commercially available monoclonal antibody, Myc

1-9E10.2, which was raised against the MYC epitope (Fig. 1B; Evan et al., 1985). The truncated P-transposase contains a nuclear localization signal (O'Kane and Gehring, 1987), but it does not have transposase activity (Karess and Rubin, 1984). The πM protein can be detected with sufficient resolution to readily distinguish individual cells in both developing and adult tissues (Fig. 1B,F,G).

In some experiments, it may be preferable to label the cell membrane rather than the nucleus. For instance, when phenotypes must be evaluated in thin sections, which do not always include the nucleus; when a second nuclear anti-
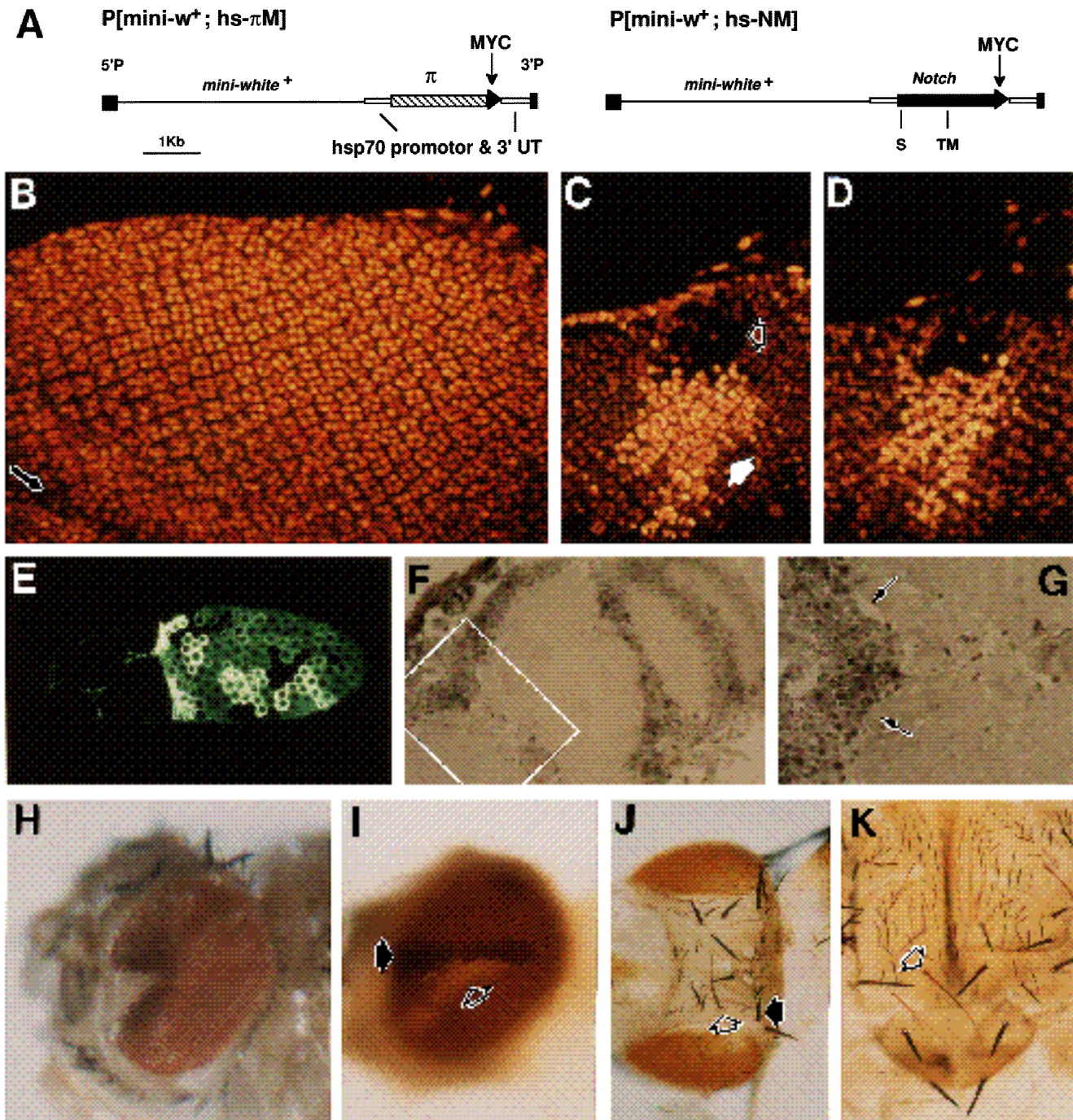

Fig. 1

gen must be scored; or when an extended cellular process like an axon must be identified; a membrane marker would be advantagous. To generate a membrane-associated cell marker, we have fused the MYC peptide to the signal peptide and the transmembrane domain of the *Drosophila* Notch protein (NM, Fig. 1A, Wharton et al., 1985); the NM protein is mainly associated with plasma and ER membranes of the cell (Fig. 1E).

The M and NM proteins, induced by heat-shock treatment, can be used to distinguish neighboring cells of different genotypes in mosaic tissues. Both markers have a short perdurance so that after a few cell divisions, marker protein induced in a cell is not detected in its descendants (Fig. 1C,E). After a brief heat shock, cells carrying zero, one or two copies of the M or NM marker genes can be distinguished from each other (Fig. 1C-E). We have repeatedly induced the expression of these proteins in multiple strains throughout development (Materials and methods). No obvious developmental defects were detected in any of these flies. To facilitate mosaic analyses for genes at different chromosomal locations, genes for these marker proteins have been placed on every major chromosome arm by P-element-mediated gene transfer (Table 1; Materials and methods).

The most obvious application of these cell markers is to mark groups of mutant cells in developing tissues so that their developmental potential can be assessed by examining their morphology and their expression of cell identity markers. Although -galactosidase (*lacZ*) has been successfully used as a cell-autonomous marker in mosaics (Wolff and Ready, 1991), we chose not to use this marker so that the expression of *lacZ* enhancer trap lines could be assayed in clones of mutant cells; enhancer trap lines provide the best differentiation and cell identity markers for many developing tissues. The different subcellular locations of the M and NM marker proteins facilitate double-labeling experiments with anti- -galactosidase or other antisera (see below). The ability to identify clones of cells carrying two copies of these cell markers in a background of cells that carry one copy of the same marker allows one both to positively mark mutant cells and to compare directly, in the same preparation, the behavior of the cells in a mutant clone with that of the cells in the corresponding wild-type twin-spot clone. This is particularly useful in analyzing mutations causing cell lethality or affecting proliferation (see below).

P[FRT] strains for producing high frequency mosaicism

In order to utilize the FRT/FLP recombination system to induce mosaicism for genes throughout the *Drosophila* genome, it is essential to generate a set of strains that each

---

Fig. 1. Cell markers for developing and adult tissues. (A) Diagrams of P-elements encoding the cell markers M and NM. The M protein is a fusion between the N-terminal 484 amino acids of the P-transposase (hatched bar) and a peptide (MYC) from the human c-myc protein (closed arrow). The NM protein is a fusion of the signal peptide (S) and transmembrane domain (TM) from the Notch protein (shaded bar) to the MYC peptide (see Materials and methods for details). These proteins are expressed under the control of the *hsp70* regulatory sequences (promoter and 3 untranslated sequences: open bars). A derivative of the *white* gene (*mini-white$^+$*; thin line) which serves as a cell-autonomous marker in the adult retina is also located within the P-element ends (black boxes). Panels B-E show confocal microscope images. (B) Expression of the M marker in a third instar larval eye imaginal disc of a *P[mini-w$^+$, hs- M]45F / +* individual. All nuclei in the disc are stained. An optical section at an apical level where the nuclei of the differentiating photoreceptor cells are located is shown; the arrow marks the position of the morphogenetic furrow (for a review of eye development see Ready, 1989). (C) An apical optical section of a mosaic third instar larval eye disc in which recombination was induced in a *w$^-$, hsFLP1; P[ry$^+$, hs-neo, FRT]43D, P[mini-w$^+$, hs- M]45F / P[ry$^+$, hs-neo, FRT]43D, +* animal. The disc was stained to visualize the M marker. A clone of cells that lack the M marker (open arrow) is accompanied by a twin-spot clone (closed arrow), which expresses the M protein at a level higher than the heterozygous background cells (also see Fig. 3B). Clones of cells that carry two copies of a marker gene are always evident in the backround of heterozygous cells carrying one copy of the same marker gene. However, cell-to-cell variations in the heat-shock response sometimes prevent the unambiguous determination of whether an individual cell carries one or two copies of the marker gene. The nuclei of polyploid cells in the peripodial membrane, seen at the top edge of the disc, are also brightly florescent. Posterior is up. (D) An optical section of the same disc shown in C at a more basal level where the nuclei of undifferentiated cells are located,

again showing the twin-spot clones. (E) Twin-spot clones of ovarian follicle cells in a stage 9 follicle were induced at the *P[ry$^+$, hs-neo, FRT]40A* element and visualized using the NM marker inserted at 31E. Note that follicle cells containing zero, one or two copies of the NM gene can be clearly distinguished. (F) Expression of the M marker inserted at 10D in the adult brain. The nuclei in the cellular cortex of the lamina, medulla and the central brain are visualized by antibody staining of a 10 μm frozen section of an adult head using an antiserum against the MYC epitope of the M marker protein and a HRP-conjugated secondary antibody. Areas of neuropil that separate these cell-rich regions are not stained. (G) An enlargement of the boxed area of F in which staining of individual nuclei within the cellular cortex (arrows) can be seen. (H) A mosaic adult eye showing a *w$^-$* clone produced by the *P[ry$^+$, hs-neo, FRT]80B* chromosome, which was marked with a P-transposon carrying a wild-type *white* gene inserted at 70C (Table 1). (I) A clone and its twin-spot clone in a mosaic adult eye of a *w$^-$, hsFLP1; P[mini-w$^+$, hs-NM]31E, P[ry$^+$, hs-neo, FRT]40A / +, P[ry$^+$, hs-neo, FRT]40A* animal. The ommatidia in both twin-spot clones are recognizable since cells in the clone that do not carry the *P[mini-w$^+$, hs-NM]* element lack any pigmentation (open arrow) while cells in the twin-spot clone carry two copies of the *P[mini-w$^+$, hs-NM]* element and have a level of pigmentation (closed arrow) higher than the background cells which carry only one copy of the same element. (J, K) Bristles of different clonal origins in the head and notum regions produced by inducing mitotic recombination in a *y $^-$, w$^-$ hsFLP1; P[ry$^+$, hs-neo, FRT]82B, Sb^{63b}, P[ry$^+$, y$^+$]96E / P[ry$^+$, hs-neo, FRT]82B , +, +* animal; the genotypes of individual bristles can be identified according to their expression of the *y$^+$* gene in the *P[ry$^+$, y$^+$]96E* element and by their expression of the *Sb^{63b}* mutation. Bristles made by cells that do not carry the *P[ry$^+$, y$^+$]* element and are homozygous for the *Sb$^+$* gene are long and yellow (open arrows). Bristles that are homozygous for the *P[ry$^+$, y$^+$]* element and the *Sb^{63b}* mutation (closed arrow) are shorter than the heterozygous background bristles.

A

P[ry⁺; hs-neo; FRT1]

B

C

Minutes of Induction
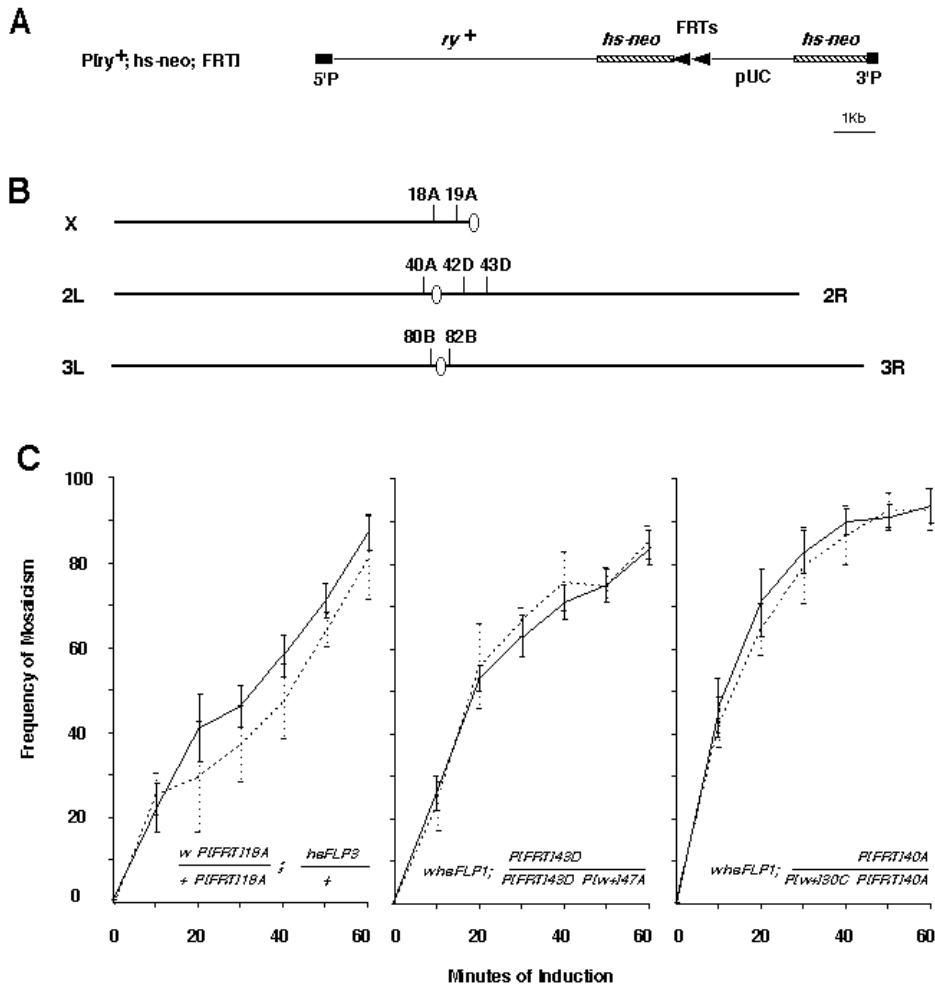
Fig. 2. (A) Diagram of the *P[ry⁺, hs-neo, FRT]* construct. The two tandem repeats of a 0.7 kb fragment containing the FRT sequence (closed arrowheads), two copies of the *hs-neo* gene (hatched bars), the 5 and 3 P-element ends (black boxes), the *rosy* gene (*ry⁺*), and the pUC vector sequences (pUC) are indicated. (B) The locations of the functional centromere-proximal *P[ry⁺, hs-neo, FRT]* insertions on the major *Drosophila* chromosome arms are illustrated; centromeres are indicated by the open circles. (C) Frequencies of mosaicism induced by recombination at various *P[ry⁺, hs-neo, FRT]* insertions with different periods of heat induction of the *hsFLP* gene. The genotypes of the animals are indicated. The frequencies of mosaicism are indicated by the percentage of eyes having at least one clone (continuous lines) and the percentages of flies having a clone(s) in one eye that also have a clone(s) in their other eye (dotted lines). Heat shock treatments of first instar larvae (30-32 hours after egg laying) were carried out for the indicated number of minutes at 38°C. A total of 13,440 eyes were scored in 5 parallel experiments; standard deviations for each heat-shock period are indicated by vertical lines with end bars.

carries an FRT sequence near the centromere of a chromosome arm. We constructed and introduced into the genome a dominantly marked FRT-containing P-element construct (*P[ry⁺, hs-neo, FRT]*, Fig. 2A). Recombination between the *P[ry⁺, hs-neo, FRT]* elements, which each contains two tandem FRT sites, occurs at high frequency in the presence of the FLP recombinase (Golic, 1991; see below). Approximately 500 lines carrying independent insertions of the *P[ry⁺, hs-neo, FRT]* element were generated and those lines that did not cause lethality or morphological defects were genetically mapped to chromosomes. The polytene chromosomal locations of 150 insertions were then determined by in situ hybridization and strains that carried a single *P[ry⁺, hs-neo, FRT]* element near the centromere of a major chromosome arm were saved.

We used the cell-autonomous eye pigmentation marker *white* (*w*) to test these FRT elements for their ability to mediate mitotic recombination between homologous chromosomes. We recombined a *w⁻* mutation onto FRT-carrying X-chromosomes and a P-transposon that carries a wild-type *w* gene (*P[w⁺]*) onto the distal part of each FRT-carrying autosomal arm. A set of strains each of which is homozygous for one of the *P[ry⁺, hs-neo, FRT]*, *P[w⁺]* arms and also carries the *hsFLP* construct on another chromosome, was generated by standard genetic

crosses (Table 1). In order to measure the frequency of *w⁻* clones in the adult eye, these strains were individually mated with a strain carrying the same *P[ry⁺, hs-neo, FRT]* insertion but without the *P[w⁺]* element. We found that most *P[ry⁺, hs-neo, FRT]* insertions let to high frequencies of mosaicism after a brief heat-shock induction of the FLP recombinase (Figs 1H, 2C; Materials and methods). In most lines, about 90% of the eyes have clones after heat-shock induction of the FLP recombinase at 38°C for 60 minutes in first instar larvae. A few *P[ry⁺, hs-neo, FRT]* insertion sites show significantly lower rates of recombination. For example, under the same experimental conditions, a *P[ry⁺, hs-neo, FRT]* insertion at polytene band 80B produced clones in only about 50% of the eyes, and an insertion at 19F produced clones in less than 1% of the eyes. The variation of the recombination frequencies for the different insertions could be due to the effects of local chromosomal structure.

There is a good correlation between the frequency of mosaicism and the duration of the heat-shock induction of the FLP recombinase (Fig. 2C), making it possible to control the frequency of mosaicism by varying the duration of the heat-shock treatment. Less than 0.1% of the *P[ry⁺, hs-neo, FRT]* animals are mosaic in the absence of the FLP recombinase gene. Without the heat-shock-induction of the FLP enzyme (at 25°C), fewer than 1% of the animals had

somatic clones (Fig. 2C). These results indicate that the *P[ry⁺, hs-neo, FRT]* chromosomes can be used to produce frequent mosaics under controlled experimental conditions.

The set of functional *P[ry⁺, hs-neo, FRT]* insertions are listed in Table 1. These insertions are close enough to the centromeres (see Fig. 2B) to allow production of individuals mosaic for more than 95% of *Drosophila* genes, as estimated from the number of map units that lie distal to these insertions (Ashburner, 1991).

When X-irradiation is used to induce mitotic recombination, radiation damage causes considerable cell death (reviewed by Ashburner, 1989). In contrast, we have not observed any obvious developmental defects associated with the induction of mosaicism using the *P[ry⁺, hs-neo, FRT]* elements. For example, among the 13,440 mosaic eyes induced by mitotic recombination in first instar larvae with three different *P[ry⁺, hs-neo, FRT]* insertions, abnormalities were detected in only five individuals, despite the
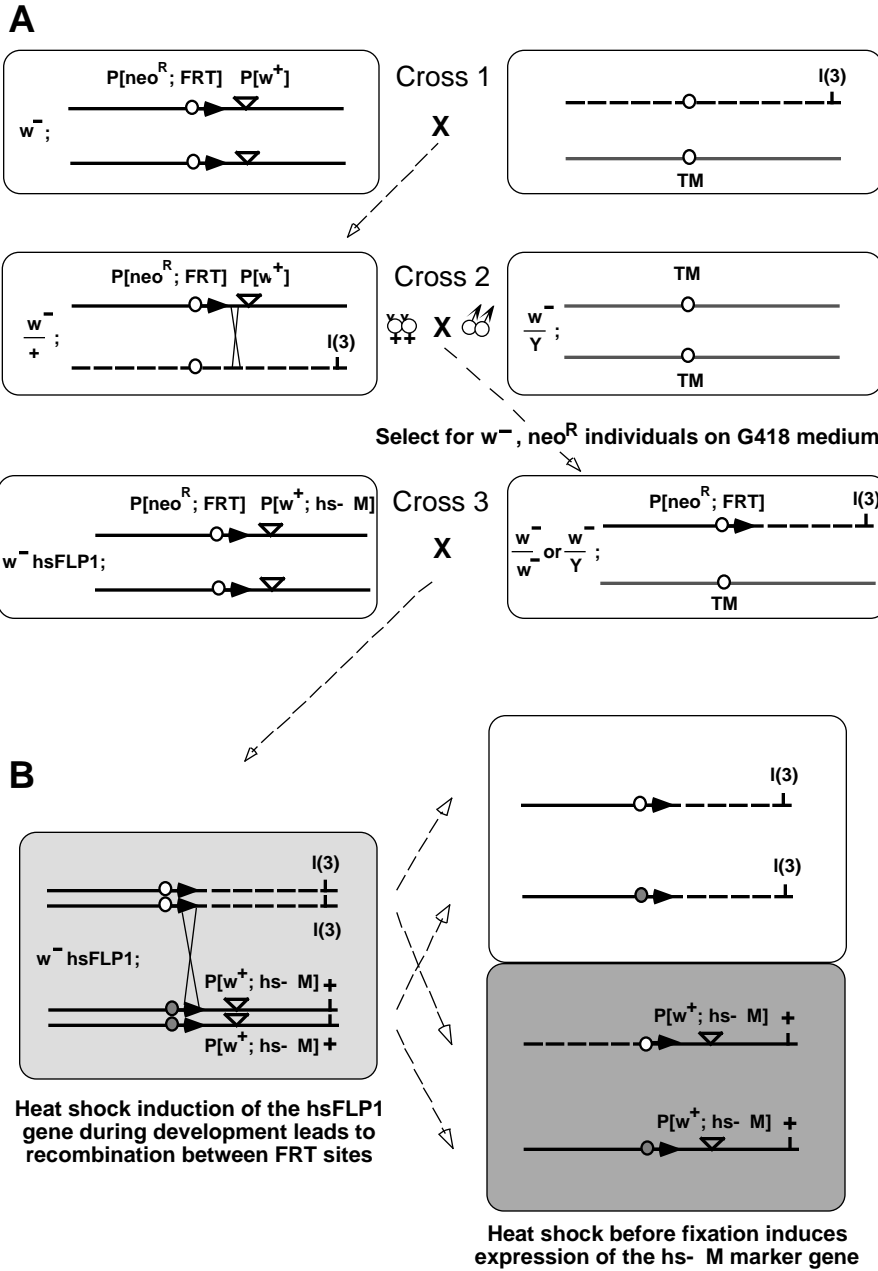
fact that approx. 90% of these eyes carried clones induced by mitotic recombination. Moreover, subsequent analysis indicated that the defects observed in these 5 individuals did not result from abnormal recombination events, but rather from the presence of spontaneous mutations causing abnormal eye phenotypes (data not shown).

FLP-induced somatic clones appear to result from a simple reciprocal recombination event between FRT sites. A mitotic recombination event in a cell heterozygous for a marker gene would produce one daughter cell with two copies of the marker and a sibling cell with no copies (Fig. 3B). Each of these daughter cells will divide to give a clone of cells in the adult (twin-spot clones). If neither cell is defective in proliferation or differentiation, the twin-spot clones will be of similar size. Examination of adults mosaic for *P[mini-w⁺, hs-NM]* (Fig. 1I, also see below), whose mosaicism was induced in first instar larvae, revealed nearby *w⁻/w⁻* and *mini-w⁺/mini-w⁺* twin-spot clones of sim-

Table 1. List of strains constructed to facilitate mosaic analysis in developing and adult *Drosophila* tissues

		FRT strains without hsFLP		FRT strains with hsFLP
	Code		Genotype	Code
X	18-1		*P[ry⁺; hs-neo; FRT]18A; ry*	18-1 F
	18-B		*B, P[ry⁺; hs-neo; FRT]18A; ry*	
	18-w		*w, P[ry⁺; hs-neo; FRT]18A*	18-w F
	18- M		*w, P[mini-w⁺; hs- M]10D, P[ry⁺; hs-neo; FRT]18A*	
	18-2 M		*w, P[mini-w⁺; hs- M]5A, 10D, P[ry⁺; hs-neo; FRT]18A*	18-2 M F
	18-NM		*w, P[mini-w⁺; hs-NM]8A, P[ry⁺; hs-neo; FRT]18A*	
	19-1		*P[ry⁺; hs-neo; FRT]19A; ry*	19-1 F
	19-y w		*y, w, P[ry⁺; hs-neo; FRT]19A*	
	19-w sn		*w, sn³, P[ry⁺; hs-neo; FRT]19A*	
2L	40-1		*P[ry⁺; hs-neo; FRT]40A; ry*	40-1 F
	40-w⁺		*w; P[ry⁺; w⁺]30C, P[ry⁺; hs-neo; FRT]40A*	40-w⁺ F
	40-y⁺		*y, w; P[ry⁺; y⁺]25F, P[ry⁺; hs-neo; FRT]40A*	40-y⁺ F
	40- M		*w; P[mini-w⁺; hs- M]36F, P[ry⁺; hs-neo; FRT]40A*	40- M F
	40-2 M		*w; P[mini-w⁺; hs- M]21C, 36F, P[ry⁺; hs-neo; FRT]40A*	40-2 M F
	40-NM		*w; P[mini-w⁺; hs-NM]31E, P[ry⁺; hs-neo; FRT]40A*	40-NM F
2R	42-1		*P[ry⁺; hs-neo; FRT]42D; ry*	42-1 F
	42-w⁺		*w; P[ry⁺; hs-neo; FRT]42D, P[ry⁺; w⁺]47A*	42-w⁺ F
	42-y⁺		*y, w; P[ry⁺; hs-neo; FRT]42D, P[ry⁺; y⁺]44B*	42-y⁺ F
	42- M		*w; P[ry⁺; hs-neo; FRT]42D, P[mini-w⁺; hs- M]45F*	42- M F
	42-NM		*w; P[ry⁺; hs-neo; FRT]42D, P[mini-w⁺; hs-NM]46F*	42-NM F
	43-2 M		*w; P[ry⁺; hs-neo; FRT]43D, P[mini-w⁺; hs- M]45F, 47F*	43-2 M F
3L	80-1		*P[ry⁺; hs-neo; FRT]80B; ry*	80-1 F
	80-w⁺		*w; P[w⁺]70C, P[ry⁺; hs-neo; FRT]80B*	80-w⁺ F
	80-y⁺		*y, w; P[ry⁺; y⁺]66E, P[ry⁺; hs-neo; FRT]80B*	80-y⁺ F
	80- M		*w; P[mini-w⁺; hs- M]75C, P[ry⁺; hs-neo; FRT]80B*	80- M F
	80-NM		*w; P[mini-w⁺; hs-NM]67B, P[ry⁺; hs-neo; FRT]80B*	80-NM F
3R	82-1		*P[ry⁺; hs-neo; FRT]82B; ry*	82-1 F
	82-w⁺		*w; P[ry⁺; hs-neo; FRT]82B, P[ry⁺; w⁺]90E*	82-w⁺ F
	82- M		*w; P[ry⁺; hs-neo; FRT]82B, P[mini-w⁺; hs- M]87E*	82- M F
	82-2 M		*w; P[ry⁺; hs-neo; FRT]82B, P[mini-w⁺; hs- M]87E, 97E*	82-2 M
	80-NM		*w; P[ry⁺; hs-neo; FRT]82B, P[mini-w⁺; hs-NM]88C*	80-NM F
	82- M Sb y⁺		*y, w; P[ry⁺; hs-neo; FRT]82B, P[mini-w⁺; hs- M]87E, Sb⁶³ᵇ, P[ry⁺; y⁺]96E*	82- M Sb y⁺ F

The strains are listed according to the chromosome arm that carries the *P[ry⁺, hs-neo, FRT]* element; each FRT-carrying arm is available with or without a *hsFLP* element on a separate chromosome. For the convenience of notation, each strain was designated by an abbreviation of its genotype. Each abbreviation starts with a number indicating the cytological location of the *P[ry⁺, hs-neo, FRT]* element. Following this number, abbreviations for the cell markers located on that FRT-carrying arm are given. A letter F is written at the end of the abbreviation if a *hsFLP* element is present in the same strain. The *w* mutation in these strains is *w¹¹¹⁸* and the *ry* allele is *ry⁵⁰⁶*. The *P[ry⁺, y⁺]* construct is described by Geyer and Corces (1987) and insertions of this ellement on the autosomes were provided by V. Corces. The genotype of the *hsFLP*-carrying strain is the same as the corresponding strain listed on the left except that it also carries the *hsFLP1* element (Golic and Lindquist, 1989) at 9F for autosomal *P[ry⁺, hs-neo, FRT]* strains or a *hsFLP* element on the *MKRS* chromosome (Chou and Perrimon, 1992) at 86E for X-linked *P[ry⁺, hs-neo, FRT]* strains; the allelism of the *ry* gene was not followed in the *hsFLP*-containing strains. To facilitate positively labeling mutant clones, two *P[mini-w⁺, hs- M]* elements which are not closely linked, were placed on each of the FRT-carrying arms except 3L. In addition, these strains express higher levels of the M marker proteins than those carrying only one copy of the marker gene and are useful in experiments that require higher levels of the M protein or shorter periods of heat-shock induction.

A

B

Heat shock induction of the hsFLP1 gene during development leads to recombination between FRT sites

Heat shock before fixation induces expression of the hs- M marker gene

Fig. 3. Diagram of the genetic crosses used to produce clones of labeled cells that are homozygous for a previously identified mutation. The relevant chromosomes are illustrated with continuous or dashed lines with their centromere shown as open circles. (A) Recombining a previously identified mutation onto an FRT-carrying chromosome arm. In order to induce clones of cells that are homozygous for a given mutation, for example, a lethal mutation on the third chromosome or *l(3)*, the *l(3)* mutation must be genetically recombined onto the distal part of the FRT-carrying arm. A strain carrying the *l(3)* mutation over a balancer chromosome (TM) is mated to a strain which is homozygous for a centromere-proximal *P[ry+, hs-neo, FRT]* element (solid arrows; indicated as P[neo^R, FRT]) on the homologous chromosome arm (cross 1). Flies carry the desired recombinant chromosome with both the *P[ry+, hs-neo, FRT]* element and the *l(3)* mutation (*P[ry+, hs-neo, FRT], l(3)*) are selected from among the progeny produced by the female progeny of cross 1 and males from a balancer stock (cross 2). Since most of the progeny of this cross will carry the parental chromosomes or unwanted recombinant chromosomes, a genetic selection scheme is used to facilitate the isolation of *P[ry+, hs-neo, FRT], l(3)* recombinants. The *hs-neo* gene in the *P[ry+, hs-neo, FRT]* construct confers resistance to G418 and can be used as a dominant selectable marker to follow the FRT sequence. To distinguish the desired recombinants from the rest of the FRT-carrying flies, we select against the distal part of the parental FRT-carrying chromosome arm. The distal part of the FRT-carrying arm has been marked with a *P[w+]* insertion (open arrows; indicated as P[w+]). Selection for *P[ry+, hs-neo, FRT], l(3)* recombinants can thus be accomplished by selecting from among the progeny of cross 2 those that are both *w*⁻ and G418 resistant (neo^R). Since these individuals are resistant to G418, they must carry the *P[ry+, hs-neo, FRT]* insertion. The *w*⁻ phenotype indicates that the *P[w+]* insertion, which is associated with the distal part of the FRT-carrying parental chromosome arm, has been recombined away from the *P[ry+, hs-neo, FRT]* insertion; thus, the resulting recombinant chromosome must have received an equivalent region from the mutation-carrying parental chromosome, and the *l(3)* mutation most likely has been recombined onto the FRT-carrying arm. For X-chromosomes, we have placed the *Bar* (*B*) mutation on the *P[ry+, hs-neo, FRT]18A* chromosome since the endogenous *w+* gene is located far away from the *P[ry+, hs-neo, FRT]18A* element; when recombining a mutation onto the *P[ry+, hs-neo, FRT]18A* chromosome, G418 resistant and non-*Bar* males are selected. The *P[mini-w+, hs- M]*, *P[mini-w+, hs-NM]* or *P[ry+, y+]* elements on the FRT-carrying chromosome arms listed in Table 1 can also be used to selectively recombine mutations onto the FRT-carrying arms in a manner analogous to that described above for the *P[w+]* elements. The recombination distances between each of the *P[ry+, hs-neo, FRT]* and *P[marker]* elements can be estimated from their cytological locations (Table 1). (B) Producing and marking clones of cells with different doses of a given mutation. After generating the recombinant chromosome that carries both the *P[ry+, hs-neo, FRT]* element and the *l(3)* mutation on the same arm, somatic clones homozygous for the *l(3)* mutation can be produced by crossing this recombinant to a strain that carries the same *P[ry+, hs-neo, FRT]* element as well as a *hsFLP* element on a separate chromosome (cross 3 in A), and then inducing mitotic recombination between FRT sequences by heat-shock induction of the FLP enzyme at the desired developmental stage in the progeny. For marking clones of cells in developing or adult tissues, the distal part of the FRT-carrying arm in the *hsFLP*-carrying strain also carries a P-transposon (open arrowheads) which contains an appropriate marker gene (for example, the M marker; illustrated as P[w+, hs- M]). Cells in a *l(3)/l(3)* mutant clone can be identified as tissues lacking the given marker (*M*⁻ *l(3)/ M*⁻ *l(3)*), while cells in the wild-type twin-spot clone (*M+ l(3)+/ M+ l(3)+*) can also be recognized by the higher level of expression of the marker gene in these cells than in the background heterozygous cells (*M+ l(3)+/ M*⁻ *l(3)*⁻). For examples of actual clones see Fig. 1.

ilar sizes, as expected if these clones were induced by a single, simple recombination event.

Mosaic analysis for a previously identified mutation

In order to use the FRT/FLP recombination system to produce clones homozygous for a previously identified mutation, the mutation of interest must be recombined onto the distal part of one of the FRT-carrying chromosome arms (Fig. 3). To facilitate identification of recombinants that acquire a distal mutation, the $P[ry^+, hs-neo, FRT]$ element was dominantly marked with the *hs-neo* gene (Steller and Pirrotta, 1985) and the distal part of each of the $P[ry^+, hs-neo, FRT]$-carrying chromosome arm was marked with a $P[w^+]$ element (w^-; $P[ry^+, hs-neo, FRT], P[w^+]$; Table 1). Recombinants that are likely to carry both the $P[ry^+, hs-neo, FRT]$ element and the mutation of interest on the same arm can be identified by selecting for both neo^R (Materials and methods) and the absence of the $P[w^+]$ element (see Fig. 3A).

Mosaic animals can be generated after crossing this recombinant to a strain that carries a chromosome arm with the same $P[ry^+, hs-neo, FRT]$ element and a cell marker as well as the *hsFLP* gene on a separate chromosome (cross 3 of Fig. 3A). The FLP recombinase is then induced in the heterozygous progeny by a brief heat-shock treatment at the developmental stage at which one wishes to induce clones (as diagrammed in Fig. 3B; Materials and methods).

To mark the resulting clones, we have placed various cell markers on each of the FRT-carrying arms. In the adult eye, the X-linked w^- gene is an excellent marker for identifying clones. For genes located on the autosomal arms, as mentioned above, we have recombined a set of the $P[w^+]$ elements onto the FRT-carrying arms (Table 1). Since the endogenous w gene on the X-chromosome is in a mutant form in these strains, the w^+ or w^- eye pigmentation phenotypes are determined by whether an autosomal arm carries a $P[w^+]$ element. In adult mosaic eyes, clones of cells that are homozygous for the parental autosomal arm that does not carry the $P[w^+]$ insert are phenotypically w^- and can be distinguished from the neighboring cells that are either homozygous or heterozygous for the $P[w^+]$-carrying homologous arm (Figs 3B, 1H). We also constructed FRT-carrying chromosomes which carry the *mini-w^+* gene (Pirrotta, 1988) as a cell-autonomous marker (w^-, *hsFLP1*; $P[ry^+, hs-neo, FRT], P[mini-w^+, hs-M \text{ or } hs-NM]$; Table 1). The *mini-$w^+$* gene produces a low level of pigmentation, and makes it possible to distinguish ommatidia in a mosaic animal which carries zero, one or two copies of the *mini-w^+* gene (Fig. 1I).

To identify clones in the rest of the adult cuticle, we placed a P-transposon that carried the wild-type *yellow* (y^+) gene ($P[ry^+, y^+]$; Geyer and Corces, 1987) onto each FRT-carrying autosomal arm (Table 1; Fig. 1J,K). The Sb^{63b} mutation, a dominant bristle marker, was also recombined onto the $P[ry^+, hs-neo, FRT]82B$-carrying arm (Table 1; Fig. 1J,K).

To identify clones in developing and internal tissues, we have recombined the M and NM cell markers onto each FRT-carrying chromosome arm (w^-, *hsFLP1*; $P[ry^+, hs-neo, FRT], P[mini-w^+, hs-M \text{ or } hs-NM]$; Table 1). These

cell markers can be used to identify clones of cells in developing or adult internal tissues (Fig. 3B; Fig. 1C-E). Since cells that are homozygous for these cell markers can be distinguished from the heterozygous background cells (Fig. 1C,E), one can also positively mark mutant cells by placing the mutation of interest onto the $P[ry^+, hs-neo, FRT]$, $P[mini-w^+, hs-M \text{ or } hs-NM]$ chromosome (see below).

A specific example: analysis of the *Egfr* gene

The *Drosophila* EGF receptor homolog gene (*Egfr*) encodes a receptor tyrosine kinase which shows a high degree of homology to mammalian EGF receptors (Shilo and Raz, 1991 review). Null mutations in the gene cause embryonic lethality (Nüsslein-Volhard et al., 1984; Price et al., 1989; Schejter and Shilo, 1989). Previous studies have shown that X-ray-induced clones of *Egfr$^-$* cells do not survive to contribute to the adult eye (Baker and Rubin, 1989). We confirmed these results using the FLP/FRT-marker strains. In addition, although no *Egfr$^-$* cells were observed, minor disruptions in the array of ommatidia were detected in many mosaic eyes (data not shown). Careful examination of the area around such disruptions revealed abnormal ommatidia with too few or two many photoreceptors (data not shown). These data suggest that clones of *Egfr$^-$* cells induced in first instar larvae survive until the third instar where they can interfere with pattern formation. Since these *Egfr$^-$* cells are unable to contribute to the adult eye, it is essential to examine the behavior of the *Egfr$^-$* cells in the imaginal eye disc to gain insight into the role of the wild-type Egfr gene in eye development.

Egfr$^-$/Egfr$^-$ clones were induced in *Egfr$^-$/Egfr$^+$* first instar larvae and the M cell marker was used to identify clones of *Egfr$^-$/Egfr$^-$* or *Egfr$^+$/Egfr$^+$* cells (Materials and methods). Both the M$^-$ Egfr$^-$/ M$^-$ Egfr$^-$ clones and their wild-type twin-spot clones (M$^+$ Egfr$^+$/ M$^+$ Egfr$^+$) are observed in the third instar larval eye discs (Fig. 4A,B,D). However, the *Egfr$^-$* clones always have many fewer cells, generally at least 10-fold fewer, than the associated wild-type twin-spot clones (Fig. 4A,B,D). This difference in clonal size has also been confirmed by placing the M marker on the *Egfr$^-$* chromosome arm. In this case, cells in the small M$^+$ Egfr$^-$/ M$^+$ Egfr$^-$ mutant clones express high levels of the M marker and cells in the large wild-type twin-spot clones (M$^-$ Egfr$^+$/ M$^-$ Egfr$^+$) do not express the M marker (Fig. 4C). Small clones could result from extensive cell death. However, the behavior of the *Egfr$^-$* cells does not resemble that of dying cells. The nuclei of these cells are not fragmented and they are able to express the M protein after heat shock (Fig. 4C). Moreover, large patches of dying cells would be expected if cell death is the primary cause of these small clones; such patches were not evident in eye discs stained with acridine orange (data not shown). Since each *Egfr$^-$* clone and its wild-type twin-spot clone are generated from a single event, the difference in clone sizes suggests the *Egfr$^-$* mutant cells do not proliferate as well as wild-type cells. Similar differences in the sizes of the *Egfr$^-$* mutant clones and their wild-type twin-spot clones are also evident in other imaginal tissues that we have examined, including the antennal, wing and leg discs (data not shown). These results suggest that Egfr is required for normal cell proliferation in all imaginal discs,

consistent with Egfr's role in cell proliferation having been conserved in vertebrate and invertebrate organisms throughout evolution.

To find out what happens to the $Egfr^-$ mutant cells during ommatidial assembly, we examined the behavior of $Egfr^-$ cells in the region posterior to the morphogenetic furrow where photoreceptor cell differentiation takes place. In this region of a wild-type eye disc, differentiating photoreceptor cells express neuronal-specific antigens, such as that

identified by an anti-HRP antibody (Jan and Jan, 1982). However, the $Egfr^-$ mutant cells do not express this neuronal antigen (Fig. 4D,I). Furthermore, while the nuclei of the differentiating photoreceptor cells rise from the basal layer, the nuclei of the developmentally uncommitted cells remain basally located in the region posterior to the furrow (Ready et al., 1976; Tomlinson, 1985). Examination of clones in this region revealed that the nuclei of the M^- $Egfr^-$/ M^- $Egfr^-$ mutant cells are basally located (Fig. 4B-
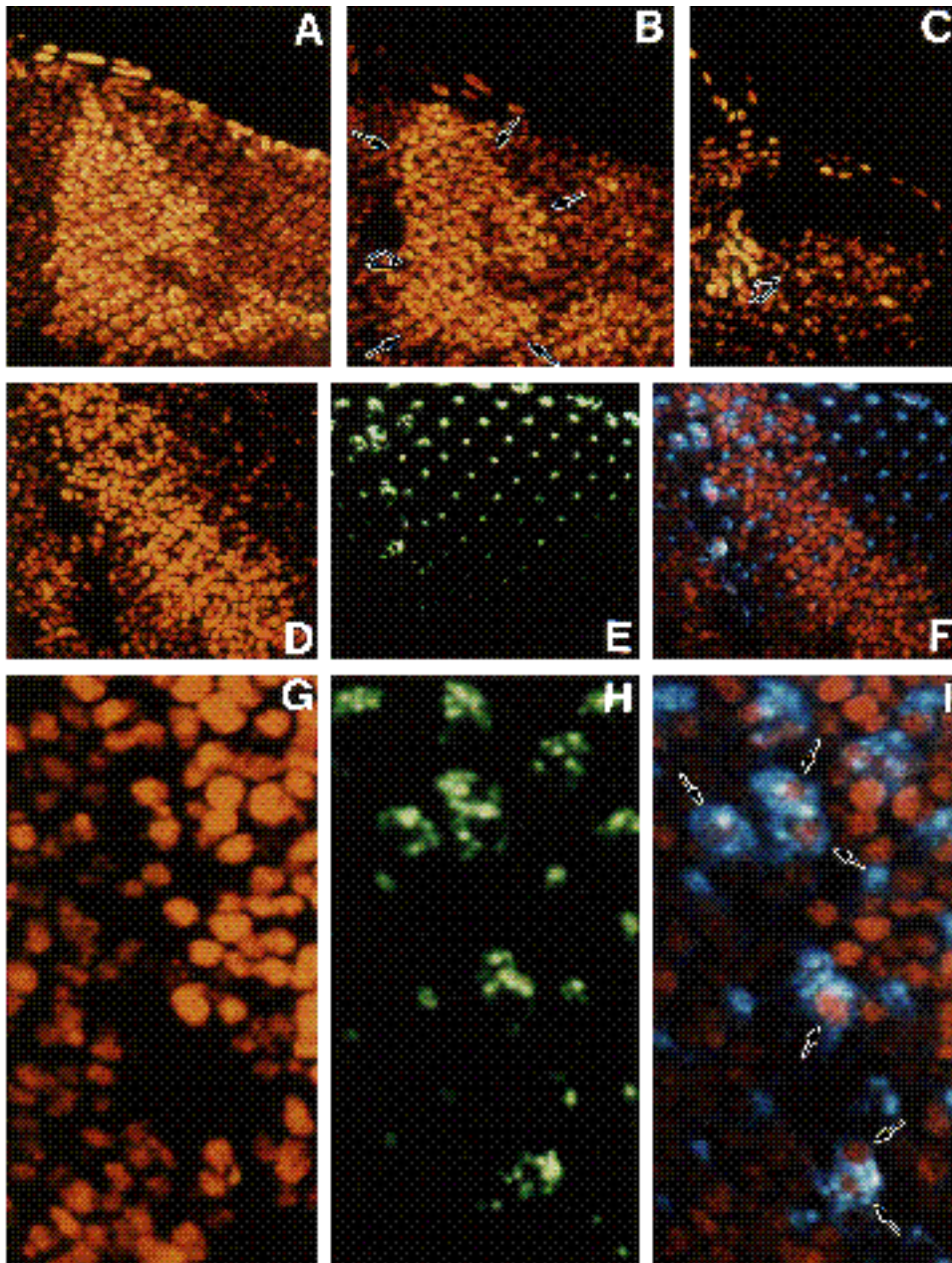
Fig. 4. $Egfr^-$ clones in developing eye discs. (A-I) Optical sections of mosaic discs in which mitotic recombination was induced in first instar larvae, stained with anti-MYC antibody (red) and anti-HRP antibody (green or blue). Posterior is up. (A) An optical section through a mosaic third instar larval eye disc at an apical level where the nuclei of the differentiating photoreceptor cells are located. Nuclei of cells of a wild-type clone (M^+ $Egfr^+$/ M^+ $Egfr^+$) are present in this focal plane and can be recognized by their intense fluorescence. In contrast, the nuclei of the cells of the $Egfr^-$ mutant twin-spot clone (M^- $Egfr^-$/ M^- $Egfr^-$) are not seen at this plane of focus. (B) A basal optical section through the same disc as in A. The nuclei of both the M^+ $Egfr^+$/ M^+ $Egfr^+$ (arrows) and the M^- $Egfr^-$/ M^- $Egfr^-$ cells (open arrow) are present at this focal plane. In a wild-type disc, nuclei located at this basal focal plane belong to the pool of uncommitted cells. The size of the $Egfr^-$ mutant clone (M^- $Egfr^-$/ M^- $Egfr^-$; open arrow and non-fluorescent nuclei) is about 20 times smaller than its wild-type twin-spot clone (M^+ $Egfr^+$/ M^+ $Egfr^+$), which can be identified because nuclei within it fluoresce brighter than those in the surrounding heterozygous background (M^+ $Egfr^+$/ M^- $Egfr^-$) cells. (C) A third instar larval eye disc. In this case, the $Egfr^-$ mutant clone (M^+ $Egfr^-$/ M^+ $Egfr^-$) was marked with two copies of the M marker (open arrow) and the M^- $Egfr^+$/ M^- $Egfr^+$ nuclei in the large wild-type twin-spot clone are non-florescent. (D) An image from another mosaic disc similar to that shown in B. (E) Optical section of the same disc at the same basal focal plane as in D stained with the anti-HRP antibody (green). In addition to the axon bundles of more apically located photoreceptor cells, which are normally present at this focal plane, some $Egfr^+$ cells adjacent to the $Egfr^-$ mutant cells are also stained with anti-HRP antibody. (F) A combination of the images in D and E. The extra neuronal cells stained with anti-HRP antibody are also stained with anti-MYC antibody, indicating that they contain the wild-type $Egfr$ gene. (G-I) Enlargements of an area in D-F, respectively. The $Egfr^+$ cells which are also stained with anti-HRP antibody (blue) are marked with arrows in I.

D). In contrast, the nuclei of cells in wild-type twin-spot clones are found at both basal and more apical levels where the nuclei of differentiating photoreceptor cells are found (Fig. 4A,B). These results suggest that *Egfr⁻* mutant cells are unable to differentiate as photoreceptor cells.

Since *Egfr⁻* mutant cells are also defective in proliferation, it is not clear whether their failure to differentiate is a direct consequence of the lack of Egfr, or a secondary effect of their abnormal proliferation. We have tried to distinguish effects on proliferation and differentiation by generating *Egfr⁻* mutant cells in the last round of mitotic division, where effects on proliferation would be irrelevant. Nevertheless, no *w⁻ Egfr⁻/w⁻ Egfr⁻* cells were found in the eyes of adults even when Flp-mediated recombination was induced in late third instar lavae (data not shown), suggesting that in addition to their effects on cell proliferation, *Egfr* mutations also interfere with differentiation.

The developmental defects seen in *Egfr⁻* cells in third instar larval eye discs provide a potential explanation for the presence in the adult of the ommatidia with too few cells. Perhaps these ommatidia were located adjacent to a clone of *Egfr⁻* cells during the assembly process in the third instar larval eye disc. Since the *Egfr⁻* cells are unable to differentiate into photoreceptor cells, there may not have been enough competent cells to form normal ommatidia. In contrast, the origin of abnormal ommatidia with too many cells is not obvious. One way to produce an ommatidium with extra wild-type photoreceptor cells is by the fusion of two developing ommatidia, which could happen if the cells separating the two developing ommatidia are *Egfr⁻* cells that ultimately do not contribute to the adult eye. Alternatively, extra photoreceptor cells could be added to an otherwise normally developing ommatidium.

To explore the origin of the ommatidia having extra photoreceptor cells, we examined the fate of wild-type cells adjacent to the *Egfr⁻* mutant clones in the third instar larval eye disc. At the base of a wild-type eye disc, the only structures that will stain with the neuronal-specific antibody anti-HRP are bundles of axons, each containing the axons from the differentiating photoreceptor cells of one ommatidium. However, at a similar basal focal plane in mosaic eye discs, in addition to these axon bundles, some cell bodies located near *Egfr⁻* mutant clones stain with the anti-HRP antibody (Fig. 4E,H), indicating the formation of ectopic neuronal cells. Overlaying the images of mosaic eye discs that were labeled with both anti-MYC and anti-HRP antibodies, shows that these ectopic neuronal cells are derived from the wild-type cells located next to *Egfr⁻* mutant cells (Fig. 4F,I). This observation supports the notion that many, if not all, of the abnormal ommatidia with extra photoreceptor cells are formed by the recruitment of extra photoreceptor cells rather than by ommatidial fusion. The fact that some of the wild-type cells next to the *Egfr⁻* mutant clones abnormally adopt a neuronal fate suggests that cells lacking Egfr can perturb the developmental fate of their neighbors.

Unlike the cell proliferation and differentiation defects, this last phenotype associated with *Egfr⁻* cells is non-autonomous. We were interested in whether such non-autonomous behavior could be observed with a gain-of-function *Egfr* mutation. The *Egfr^E* mutation is thought to be a hypermorphic allele of the *Egfr* gene, since deletion of *Egfr* suppresses the dominant rough eye phenotype of *Egfr^E* (Baker and Rubin, 1989, 1992). While the number of the ommatidia in an *Egfr^E/+* eye resembles that of a wild-type eye, very few ommatidia are formed in an *Egfr^E/Egfr^E* eye, indicating that the increased Egfr activity in *Egfr^E* suppresses the differentiation of ommatidia (Baker and Rubin, 1989). We addressed the question of non-autonomy by generating a clone of *Egfr^E/Egfr^E* cells in a background of *Egfr^E/+* cells, and asking whether they develop
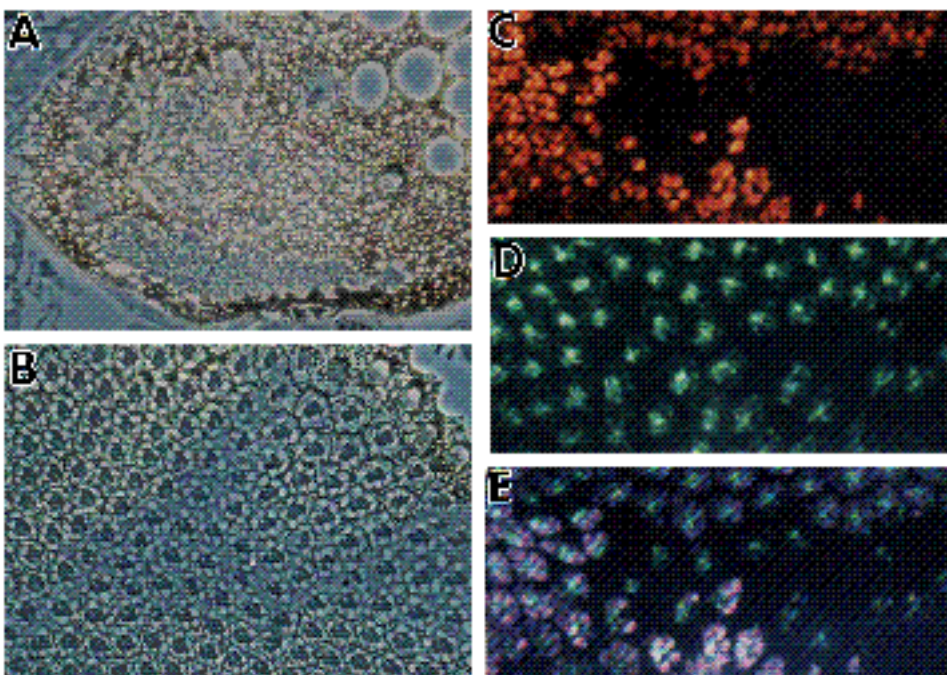

Fig. 5. *Egfr^E* clones in the adult eye and developing eye imaginal disc. (A) A section through an *Egfr^{EB1}/Egfr^{EB1}* eye. Only about 30 ommatidia are seen. (B) A section through a mosaic eye in which a clone of *Egfr^{EB1}/Egfr^{EB1}* cells (unpigmented) was induced by mitotic recombination during the first larval instar in an *Egfr^{EB1}/+* background. Many *Egfr^{EB1}/Egfr^{EB1}* ommatidia have developed. (C) An optical section of a portion of a mosaic third instar larval eye disc showing a *M⁻ Egfr^{EB1}/ M⁻ Egfr^{EB1}* clone in a *M⁺ +/ M⁻ Egfr^{EB1}* background stained with anti-MYC antibody (red). Posterior is up. (D) Optical section of the anti-HRP staining (green) of the same disc at the same focal plane as in C. (E) A combination of the images shown in C and D. Many ommatidia develop in the *Egfr^{EB1}/Egfr^{EB1}* clone adjacent to the *Egfr^{EB1}/+* or +/+ cells.

differently from $Egfr^E/Egfr^E$ cells in an $Egfr^E/Egfr^E$ eye. Interestingly, not only are there ommatidia in the w^- $Egfr^E/w^-$ $Egfr^E$ clones, but many of these clones contain more ommatidia than are seen in an entire $Egfr^E/Egfr^E$ eye (compare Fig. 5A with B). This observation indicates that the $Egfr^E/Egfr^E$ cells are somehow rescued for ommatidial differentiation by the surrounding $Egfr^E/+$ or $+/+$ tissues. We have further confirmed this finding by directly observ-

ing such $Egfr^E/Egfr^E$ clones in third instar larval eye discs. As revealed by anti-MYC and anti-HRP double staining, many ommatidia form within the $Egfr^E/Egfr^E$ clones, especially in the regions adjacent to $Egfr^E/+$ or $+/+$ tissues (Fig. 5C-E). These data are consistent with the behavior of the loss-of-function $Egfr$ mutant cells; in both cases, cells are more likely to differentiate as photoreceptors if they are in contact with cells with lower Egfr activities.
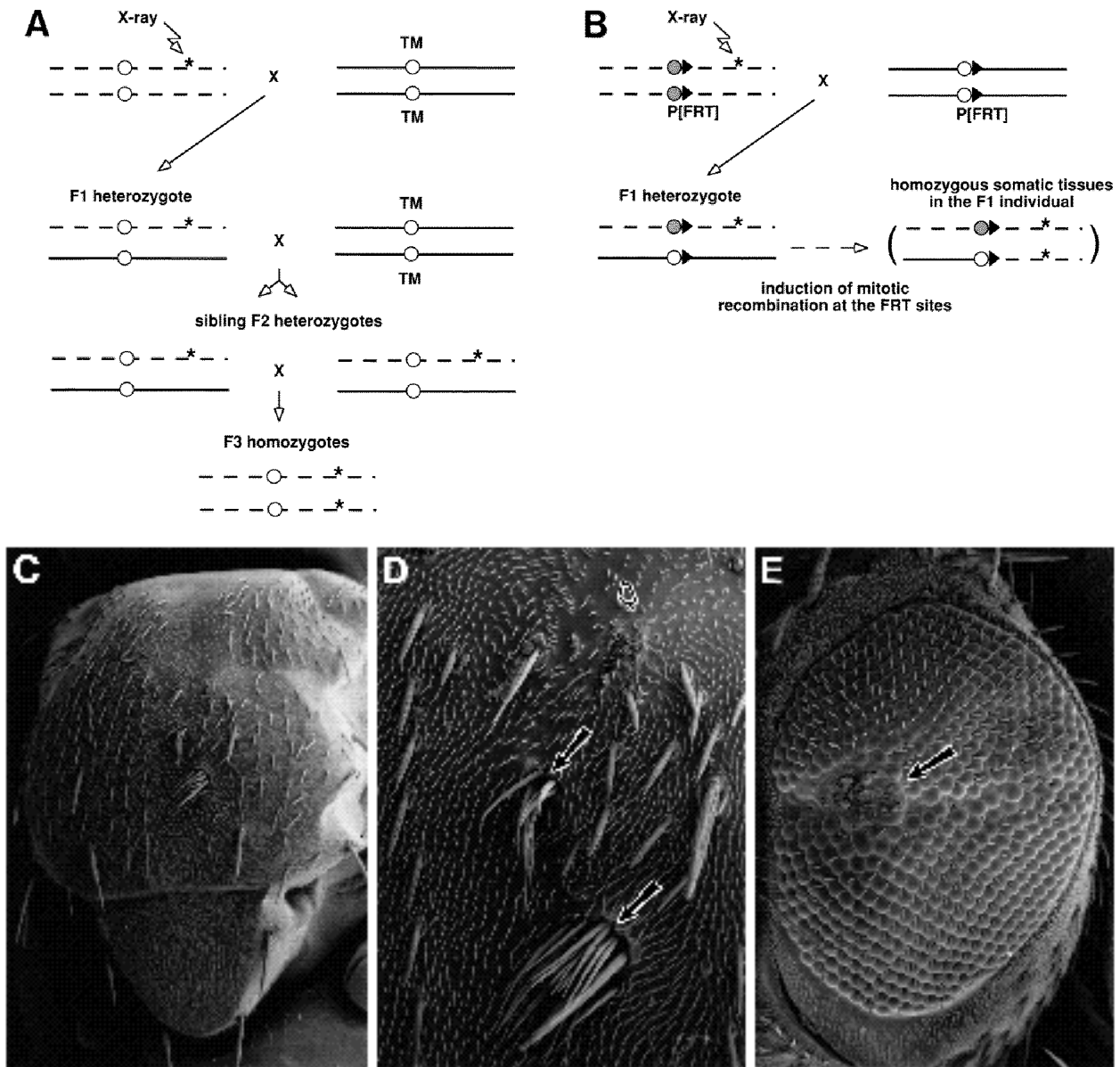
Fig. 6. (A) Diagram of a standard F_2 genetic screen. A recessive mutation (*) induced in the germline of the parent is identified in homozygous flies of individual lines that are generated from three generations of crosses. TM, balancer chromosome. (B) Using a strain having a *P[FRT]* element inserted near the centromere of a chromosome arm, induced recessive mutations on that arm can be identified in F_1 heterozygous individuals by producing and examining somatic clones of cells that are homozygous for the mutagenized chromosome arm. (C) Phenotypes of clones on the notum of an F_1 individual that was identified in a screen carried out as diagrammed in B for mutations on the right arm of the third chromosome. (D) An enlargement of part of C. Clones of cells that are homozygous for this *Delta* mutation, Dl^{82-23}, produce no bristle structures (open arrows) or multiple bristles (close arrows). (E) Clones that are homozygous for *Dl* mutations form highly disordered tissues in the eye (arrow). Clones that are mutant for a previously isolated *Dl* allele, Dl^{10G114} (Jürgens et al., 1984), produced similar bristle and eye phenotypes (data not shown).

Using the P[FRT], P[marker] strains for F₁ genetic screens

The genetic screens carried out by Nüsslein-Volhard and Wieschaus (1980) for embryonic lethal mutations affecting the pattern of the larval cuticle proved to be extremely informative. However, systematic screens for lethal mutations affecting the development and function of adult structures have not been possible. The development and function of adult organs requires genetic information from a large number of genes. Many of these genes also play essential roles during early development and consequently animals that lack them often die at early developmental stages. Genetic screens that identify mutations by examining mutant phenotypes in homozygous animals, are not only biased against such mutations, but also are laborious, since they require the generation of individual lines of homozygous animals. Although it has been appreciated that lethal mutations affecting adult structures could be identified in mosaics (Garcia-Bellido and Dapena, 1974), the low frequency of mosaicism induced by traditional methods (e.g. X-irradiation) made such an approach impractical for systematic screens. The high frequency of mosaicism that can be produced for most of the genome using the strains that we have generated provides a powerful way to screen for new mutations that affect the development and function of many tissues. A standard genetic screen for recessive mutations affecting a given structure involves examination of homozygous animals from individual lines generated by three generations of crosses (an F₂ screen; Fig. 6A). Instead of isolating mutations in homozygous animals, mutations can be identified by examining clones of mutant tissues within heterozygous animals. Thus screens utilizing the FRT-carrying strains can identify phenotypes in a single generation (F₁ screens) as opposed to the three generations required in a standard F₂ screen (Fig. 6B). Furthermore, standard F₂ screens for recessive mutations affecting the structure or function of the adult are strongly biased against genes in which loss-of-function mutations decrease viability. In contrast, F₁ screens that involve examining mosaic mutant tissues in heterozygous animals should allow even lethal mutations to be recovered.

Table 2. An F₁ genetic screen for mutations affecting the adult cuticular structures in the eye and on the notum

Total number of the F₁ animals scored:	5514
Number of the mutant F₁ mosaics identified:	49(1%)
Number of the mutant F₁ mosaics that are fertile:	46
Number of the mutations that breed true:	42(86%)
Mutations affecting both eye and notum:	14
Mutations affecting eye only:	20
Mutations affecting notum only:	8

Mutations affecting the adult cuticular structures that were isolated in an F₁ screen for the right arm of the third chromosome. F₁ offspring were examined under a dissecting microscope for abnormalities in the eye (roughness or scars) or on the notum (missing or duplicating bristles) that were associated with somatic clones. About 90% of the F₁ individuals had clones in adult cuticle. From the fact that six of the mutations are on viable chromosomes, we estimated that the X-irradiation induced an average of one lethal mutation per chromosome arm in this screen.

To test the feasibility of identifying mutations in homozygous clones in F₁ heterozygous animals, we performed a pilot screen for mutations on the right arm of the third chromosome that affect adult cuticular tissues. Since common chemical mutagens such as ethyl methane sulfonate (EMS) usually modify only one of the two DNA strands, mutations whose phenotypes are observed in somatic tissues after treatment with chemical mutagens are not always transmitted in the germline (reviewed by Ashburner, 1989). We used X-irradiation as a mutagen, because the mutagenic events induced by X-irradiation usually involve both strands of the DNA duplex, and thus both the soma and germline cells will carry the same mutation (reviewed by Ashburner, 1989). We looked for clones in F₁ individuals which were homozygous for the *P[ry⁺, hs-neo, FRT]82B* element and heterozygous for both the mutagenized chromosome and the *P[mini-w⁺; hs- M]87E* element (progeny of a cross between mutagenized *82-1 F* males and *82- M Sb y⁺ F* females; Table 1; Materials and methods). These F₁ individuals also carried the *Sb⁶³ᵇ* mutation and a *P[ry⁺, y⁺]* element on the *P[ry⁺, hs-neo, FRT]82B*, *P[mini-w⁺; hs- M]87E* chromosome arm. Together, these markers allow us to assess the phenotype and genotype of the majority of adult cuticular structures in the same screen. Moreover, we can identify both the *w⁻* clones that are homozygous for the mutagenized chromosome arm and the wild-type *mini-w⁺/mini-w⁺* twin-spot clones, which are more darkly pigmented than the surrounding tissue. Clones of cells that are mutant for genes that are important for cell proliferation, cell fate determination, and differentiation often give no adult cuticle. However, the presence of darkly pigmented *mini-w⁺/mini-w⁺* clones that are not accompanied by *w⁻* twin-spot clones reveals the presence of such mutations. About 5,000 F₁ mosaic adults were examined; 49 (1%) of the F₁ individuals were found to carry clones that displayed abnormal cuticular structures in the eye or on the notum (Table 2; Materials and methods). Forty-two (86%) of the mutations responsible for these clonal phenotypes were recovered in the next generation; both viable and lethal mutations were recovered. Two mutations whose homozygous tissues form no adult structures were also identified in the screen. One of the 42 mutations is a new *Delta* (*Dl*) allele. The cuticular phenotypes of this allele are shown in Fig. 6C-E. In conclusion, the results of our pilot screen suggest that such F₁ screens are an efficient, effective and unbiased way to isolate mutations affecting many biological processes.

REFERENCES

Ashburner, M. (1989). Drosophila *A Laboratory Handbook.* Cold Spring Harbour: Cold Spring Harbor Laboratory Press.

Ashburner, M. (1991). *Drosophila* genetic maps. *Drosophila Inf. Service* **69,** 1-399.

Baker, N. E. and Rubin, G. M. (1989). Effect on eye development of dominant mutations in *Drosophila* homologue of the EGF receptor. *Nature* **340,** 150-153.

Baker, N. E. and Rubin, M. G. (1992). *Ellipse* mutations in the *Drosophila* homologue of the EGF receptor affect pattern formation, cell division, and cell death in eye imaginal discs. *Dev. Biol.* **150,** 381-396.

Chou, T.-B. and Perrimon, N. (1992). Use of a yeast site-specific recombinase to produce female germline chimeras in *Drosophila*. *Genetics* **131,** 643-653.

Clifford, R. J. and Schüpbach, T. (1989). Coordinately and differentially mutable activities of *torpedo*, the *Drosophila* melanogaster homolog of the vertebrate EGF receptor gene. *Genetics* **123,** 771-787.

Evan, G. I., Lewis, G. K., Ramsay, G. and Bishop, J. M. (1985). Isolation of monoclonal antibodies specific for human c-myc proto-oncogene product. *Mol. Cell. Biol.* **5,** 3610-3616.

Fortini, M. E. and Rubin, G. M. (1990). Analysis of *cis*-acting requirements of the *Rh3* and *Rh4* genes reveals a bipartite organization to rhodopsin promoters in *Drosophila melanogaster*. *Genes Dev.* **4,** 444-463.

Friesen, H. (1936). Spermatogoniales Crossing-over bei Drosophila. *Z. Indukt. Abstammungs. Vererbungsl.* **71,** 501-526.

Garcia-Bellido, A. and Dapena, J. (1974). Induction, detection and characterization of cell differentiation mutants in *Drosophila*. *Mol. Gen. Genet.* **128,** 117-130.

Garcia-Bellido, A. and Merriam, J. R. (1969). Cell lineage of the imaginal discs in Drosophila gynandromorphs. *J. Exp. Zool.* **170,** 61-75.

Geyer, P. K. and Corces, V. G. (1987). Separate regulatory elements are responsible for the complex pattern of tissue-specific and developmental transcription of the yellow locus in Drosophila melanogaster. *Genes Dev.* **1,** 996-1004.

Golic, K. G. (1991). Site-specific recombination between homologous chromosomes in *Drosophila*. *Science* **252,** 958-961.

Golic, K. G. and Lindquist, S. (1989). The FLP recombinase of yeast catalyzes site-specific recombination in the *Drosophila* genome. *Cell* **59,** 499-509.

Hall, J. C., Gelbart, W. M. and Kankel, D. R. (1976). Mosaic system. In *The Genetics and Biology of* Drosophila. (ed. M. Ashburner and E. Novitski) vol. 2a. pp. 265-308. New York: Academic Press.

Hopp, T. P., Prickett, K. S., Price, V. L., Libby, R. T., March, C. J., Cerretti, D. P., Urdal, D. L. and Conlon, P. J. (1988). A short polypeptide marker sequence useful for recombinant protein identification and purification. *Bio. Technol.* **6,** 1204-1210.

Hotta, Y. and Benzer, S. (1972). Mapping of behaviour in Drosophila mosaics. *Nature* **240,** 527-535.

Jan, L. Y. and Jan, Y. N. (1982). Antibodies to horseradish peroxidase as specific neuronal markers in *Drosophila* and grasshopper embryos. *Proc. Natl. Acad. Sci. USA* **79,** 2700-2704.

Janning, W. (1972). Aldehyde-oxidase as a cell marker for internal organs in Drosophila melanogaster. *Naturwissenschaften* **59,** 516-517.

Jürgens, G., Wieschaus, E., Nüsslein-Volhard, C. and Kluding, H. (1984). Mutations affecting the pattern of the larval cuticle in Drosophila melanogaster. II. Zygotic loci on the third chromosome. *Roux's Arch Dev. Biol.* **193,** 283-295.

Kankel, D. R. and Hall, J. C. (1976). Fate mapping of nervous system and other internal tissues in genetic mosaics of Drosophila melanogaster. *Dev. Biol.* **48,** 1-24.

Karess, R. E. and Rubin, G. M. (1984). Analysis of P transposable element functions in Drosophila. *Cell* **38,** 135-146.

Lawrence, P. A. (1981). A general cell marker for clonal analysis of *Drosophila* development. *J. Embryol. Exp. Morph.* **64,** 321-332.

Lawrence, P. A., Johnston, P. and Morata, G. (1986). Methods of marking cells. In Drosophila*: A Practical Approach* (ed. D. B. Roberts), pp. 229-242. Oxford: IRL Press.

Lindsley, D. L. and Zimm, G. G. (1992). *The Genome of* Drosophila melanogaster. San Diego: Academic Press.

Lis, J. T., Simon, J. A. and Sutton, C. A. (1983). New heat shock puffs and beta-galactosidase activity resulting from transformation of *Drosophila* with an hsp70-lacZ hybrid gene. *Cell* **35,** 403-410.

McLeod, M., Volkert, F. and Broach, J. (1984). Components of the site-specific recombination system encoded by the yeast 2-micro circle. *Cold Spring Harbor Symp. Quant. Biol.* **49,** 779-787.

Morgan, T. H. (1914). Mosaics and gynandromorphs in *Drosophila*. *Proc. Soc. Exp. Biol. Med.* **11,** 171-172.

Nüsslein-Volhard, C. and Wieschaus, E. (1980). Mutations affecting segment number and polarity in *Drosophila*. *Nature* **287,** 795-801.

Nüsslein-Volhard, C., Wieschaus, E. and Kluding, H. (1984). Mutations affecting the pattern of the larval cuticle in *Drosophila melanogaster*. I. Zygotic loci on the second chromosome. *Roux's Arch. Dev. Biol.* **193,** 267-282.

O'Hare, K. and Rubin, G. M. (1983). Structures of P transposable elements and their sites of insertion and excision in the *Drosophila melanogaster* genome. *Cell* **34,** 25-35.

O'Kane, C. J. and Gehring, W. J. (1987). Detection in situ of genomic regulatory elements in Drosophila. *Proc. Natl. Acad. Sci. USA* **84,** 9123-9127.

Patterson, J. T. (1929). The production of mutations in somatic cells of *Drosophila melanogaster* by means of X-rays. *J. Exp. Zool.* **53,** 327-372.

Pirrotta, V. (1980). Vectors for P-element transformation in *Drosophila*. In *Vectors. A Survey of Molecular Cloning Vectors and their Uses* (ed. R. L. Rodriguez and D. T. Denhardt), pp. 437-456. Boston and London: Butterworths.

Postlethwait, J. H. (1976). Clonal analysis of Drosophila cuticular patterns. In *The Genetics and Biology of* Drosophila. (ed. M. Ashburner and T. R. F. Wright) vol. 2c, pp. 359-441. New York: Academic Press.

Price, J. V., Clifford, R. J. and Schüpbach, T. (1989). The maternal ventralizing locus *torpedo* is allelic to *faint little ball*, an embryonic lethal, and encodes the *Drosophila* EGF receptor homolog. *Cell* **56,** 1085-1092.

Ready, D. F. (1989). A multifaceted approach to neural development. *Trends Neurosci.* **12,** 102-110.

Ready, D. F., Hanson, T. E. and Benzer, S. (1976). Development of the *Drosophila* retina, a neurocrystalline lattice. *Dev. Biol.* **53,** 217-240.

Rebay, I., Fleming, R. J., Fehon, R. G., Cherbas, L., Cherbas, P. and Artavanis-Tsakonas, S. (1991). Specific EGF repeats of Notch mediate interactions with Delta and Serrate: Implications for Notch as multifunctional receptor. *Cell* **67,** 687-699.

Rio, D. C., Laski, F. A. and Rubin, G. M. (1986). Identification and immunochemical analysis of biologically active Drosophila P element transposase. *Cell* **44,** 21-32.

Rubin, G. M. (1985). P transposable elements and their use as genetic tools in *Drosophila*. *Trends Neurosci.* **6,** 231-233.

Rubin, G. M. and Spradling, A. C. (1982). Genetic transformation of *Drosophila* with transposable element vectors. *Science* **218,** 348-353.

Schejter, E. D. and Shilo, B.-Z. (1989). The *Drosophila* EGF receptor homolog (DER) gene is allelic to *faint little ball*, a locus essential for embryonic development. *Cell* **56,** 1093-1104.

Shilo, B.-Z. and Raz, E. (1991). Developmental control by the Drosophila EGF receptor homolog DER. *Trends Genet.* **7,** 388-392.

Spradling, A. C. and Rubin, G. M. (1983). The effect of chromosomal position on the expression of the *Drosophila* xanthine dehydrogenase gene. *Cell* **34,** 47-57.

Steller, H. and Pirrotta, V. (1985). A transposable P vector that confers selectable G418 resistance to *Drosophila* larvae. *EMBO J.* **4,** 167-171.

Stern, C. (1936). Somatic crossing over and segregation in *Drosophila melanogaster*. *Genetics* **21,** 625-730.

Thummel, C. S. and Pirrotta, V. (1992). New pCaSpeR P element Vectors. *Drosophila Inf. Service* **71,** 150.

Tomlinson, A. (1985). The cellular dynamics of pattern formation in the eye of *Drosophila*. *J. Embryol. Exp. Morph.* **89,** 313-331.

Wharton, K. A., Johansen, K. M., Xu, T., and Artavanis-Tsakonas, S. (1985). Nucleotide sequence from the neurogenic locus notch implies a

gene product that shares homology with proteins containing EGF-like repeats. *Cell* **43,** 567-581.

Wolff, T. and Ready, D. F. (1991). The beginning of pattern formation in the *Drosophila* compound eye: The morphogenetic furrow and the second mitotic wave. *Development* **113,** 841-850.

Xu, T. and Artavanis-Tsakonas, S. (1990). *deltex*, a locus interacting with the neurogenic genes, *Notch, Delta* and *mastermind* in *Drosophila melanogaster*. *Genetics* **126,** 665-677.